EFFECTS OF SHEAR STRESS IN TELETACTION AND HUMAN PERCEPTION *

G. Moy and R.S. Fearing
Department of Electrical Engineering and Computer Science
University of California
Berkeley, CA 94720-1770

ABSTRACT

Ideally, a tactile stimulator presents information through control of surface normal stress and surface shear stresses. Psychophysical experiments measured the effect of shear stress information on the perception of static stimuli applied normal to the surface. Wax gratings in two different orientations and various spatial frequencies were used as stimuli. Elastic layers, representing the anti-aliasing filter on a tactile display, were placed over the stimuli. Using an elastic layer which reduces shear stress transmission improved perception compared to standard elastic layers. Spatial resolution differences due to different elastic layers are explained by modulation indices determined from the predicted sub-surface strain using an elastic half-plane model.

INTRODUCTION

Information about texture, local compliance, and local shape is important in applications such as telesurgery or handling of fragile objects in telerobotics. Figure 1 shows a general configuration of a teletaction system. One possible application is on a robotic laparoscopic telesurgery system. The tactile sensor is mounted on the end effector (the laparoscopic instrument), and the tactile stimulator display is mounted on the master manipulator (the user interface). The tactile stimulator presents information recorded by the tactile sensor to the user. Ideally, the patterns felt by the user would be indistinguishable from direct contact with the environment. The tactile stimulator needs to generate surface stresses that realistically represent data collected by the tactile sensor. To fully control surface stress, the ideal tactile display system would be an infinite density array of 3 DOF actuators. This paper examines the perceptual difference between a 1 DOF and 3 DOF tactile display for simple grating patterns.

Tactile displays can control either displacements or forces. In a displacement display, an array of pins is shaped into a contour. In a force display, the pin array will produce a surface stress distribution representing the data. For a force display, we examine the effects of reducing the amount of shear stress information transmitted. As seen in the Sensopad[1], a device to aid in breast self examinations, reduction of shear stress can enhance detection of embedded objects. Similarly, there is enhanced detection of surface roughness when a piece of paper, used to reduce shear, was placed between a finger and sandpaper (Lederman 1978).

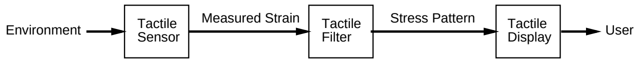

Figure 1: A block diagram representation of a teletaction system.

Most tactile display systems use an array of actuated 1 DOF pins to stimulate the slowly adapting afferent (SA I) units. Tactile display designs have used solenoids (Fischer et al, 1995), shape memory alloys (Howe et al 1995; Hasser and Daniels 1996), pneumatics (Cohn et al 1992), electrostatics (Beebe et al 1995), and tangential tactors using linear microactuators (Ghodssi et al 1996). Electrocutaneous stimulation (Kaczmarek et al 1991) is mechanically quite simple; however, the perceptual effects are hard to analyze. We are unaware of any tactile display sytem with an array of actuated 3 DOF pins.

The density of the stimulator array is limited by actuator size. Currently, the spacing between the centers of the pins is around 2 mm (Cohn et al 1992; Howe et al 1995). The array is covered by an elastic layer which functions as an anti-aliasing filter. Without the anti-aliasing filter, the user would feel an array of pins instead of a smooth continuous surface. Until actuator technology advances to the point where pin density equals mechanoreceptor density, an anti-aliasing filter will still be needed. Even when actuator densities are high enough,

*This work was funded in part by: NSF grant IRI-9531837.

[1] Inventive Products, Inc., Decatur, IL

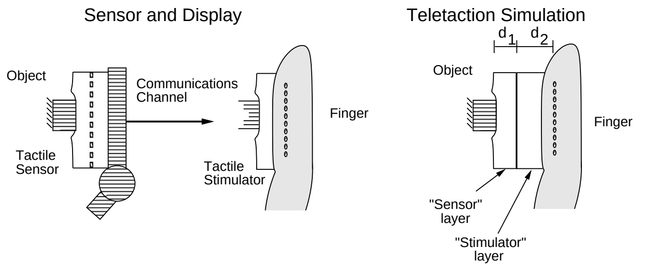

Figure 2: Teletaction with a) a sensor and display, b) elastic layers

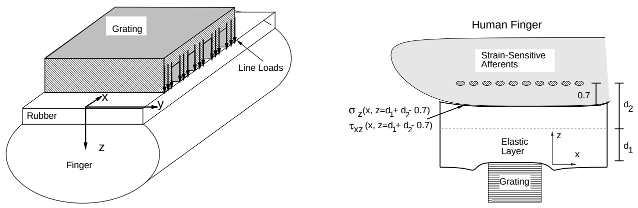

Figure 3: a) Finger and stimuli geometry for plane stress assumption b) slice of the x-z plane

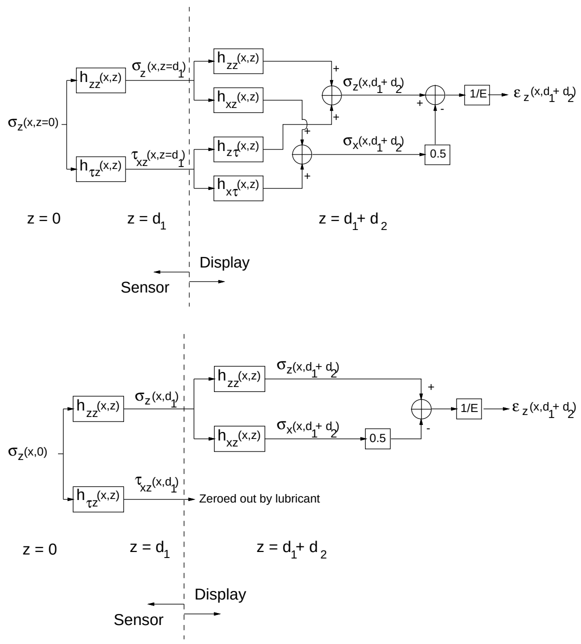

Figure 4: Block diagrams of the system with two 1 mm sheets of rubber with a) no lubricant, b) lubricant between the rubber layers

an elastic layer will still be needed to protect users from the small display pins stabbing into the skin.

Human tactile perception is not as well understood as the human vision system. Some areas, such as human tactile sensing sensitivity, sensor density, and spatial and temporal frequency response have been studied (Phillips and Johnson 1981; Loomis and Lederman 1986; Shimojo et al 1997; Tan 1995; Singh 1997).

The teletaction problem can be split into three parts, a sensor side, a stimulator side, and a communications channel (Figure 2) (Fearing et al 1997). In our case, the communications channel is a direct contact between the sensor and the stimulator to avoid aliasing problems. The sensor is represented by one elastic layer, and the display is represented by another elastic layer. By controlling the boundary conditions between the "sensor" layer and the "stimulator" layer, we can physically simulate 1 DOF and 3 DOF tactile displays. We assume that contact stresses are not affected by this subsurface boundary change. We test human perception of gratings to determine if an array of 1 DOF actuators would be as effective as an array of 3 DOF actuators.

One of the elastic layer combinations consists of two 1 mm thick pieces of silicone rubber (Dow Corning's HSII). Assuming perfect adhesion at the boundary between layers, full normal and shear stress information is transmitted between the tactile sensor and display. The other elastic layer combination consists of two 1 mm thick pieces of HSII with a thin layer of lubricant between them. Full normal stress information but reduced shear stress information is transmitted between the tactile sensor and display.

MODEL OF THE TELETACTION SYSTEM

In this section, we describe a model of the interactions between the human finger and normally indented stimuli. For simplicity, we use the plane-stress approximation (Figure 3a), and assume that the finger senses subsurface normal strain; higher order and more realistic models of the finger are being developed by others, such as (Srinivasan and Dandekar 1996). We first present the geometry and mechanics of the system. We then model the system with transfer functions.

For our teletaction model, stimuli are transmitted through two rubber layers to the finger. The two rubber layers represent the tactile sensor and display (Figure 2b). We want to model the normal strain due to indentations from the stimuli with the two different boundary conditions between the rubber layers. In the first case, the rubber layer is two 1 mm sheets of rubber. The block diagram for the first case is represented in Figure 4a. In the second case, we use two 1 mm sheets of rubber with a lubricant between the layers, and is represented in Figure 4b. This lubricant has the effect of reducing (and in the ideal case, zeroing) the shear stress from the first layer to the second layer.

For a basic model of the sensor, stimulator, and finger, we use the half-plane elastic analysis of Phillips and Johnson (1981) as a starting point. The plane stress assumption is used for our analysis since it is similar to the response of mechanoreceptors in the fingers of macaque monkeys (Phillips and Johnson 1981).

The indentations presented to the finger by the stimuli are represented as line loads applied to the rubber layer. These line loads are constant along the y-axis, but vary along the x-axis. For planar stress analysis, we use a thin slice of the x-z plane (Figure 3b).

Starting with the stresses in a slice for a line load applied at the surface (Johnson 1985), the normal strain at depth z due to a line load with normal component P and tangential component Q is:

$$\begin{aligned}\epsilon_z &= \epsilon_{zp} + \epsilon_{zq} = \frac{1}{E}(\sigma_{zp} - \nu\sigma_{xp}) + \frac{1}{E}(\sigma_{zq} - \nu\sigma_{xq}) \\ &= \frac{-2Pz}{\pi E r^4}(z^2 - \nu x^2) + \frac{-2Qxz}{\pi E r^4}(z - \nu x) \\ &= \frac{-2z}{\pi E r^4}[P(z^2 - \nu x^2) + Q(xz - \nu x^2)]\end{aligned}$$

where $E = 4 \times 10^5$ N/m^2 and $\nu = 0.5$. This is not what the human feels, but is a good first order approximation and easy to calculate. For this model, we will naively assume that the finger and rubber stiffnesses are equal. The elastic modulus of skin varies nonlinearly with the applied load.

We assume a normal frictionless indentation, so there will be no shear force applied at the contact surface between the stimuli and rubber, i.e. $\tau_{xz}(x, z = 0) = 0$. The relations of the blocks from Figure 4, based on line load equations are:

$$\begin{aligned}h_{zz}(x,z) &= \frac{-2z^3}{\pi r^4}, H_{zz}(s,z) = -2\pi z e^{-2\pi z s}(\frac{1}{2\pi z} + s), \\ h_{xz}(x,z) &= \frac{-2x^2 z}{\pi r^4}, H_{xz}(s,z) = -2\pi z e^{-2\pi z s}(\frac{1}{2\pi z} - s), \\ h_{\tau z}(x,z) &= \frac{-2xz^2}{\pi r^4}, H_{\tau z}(s,z) = j2\pi z s e^{-2\pi z s}, \\ h_{z\tau}(x,z) &= \frac{-2xz^2}{\pi r^4}, H_{z\tau}(s,z) = j2\pi z s e^{-2\pi z s}, \\ h_{x\tau}(x,z) &= \frac{-2x^2 z}{\pi r^4}, H_{x\tau}(s,z) = j(2 - 2\pi z s)e^{-2\pi z s},\end{aligned}$$

where z is the depth of interest, $s \geq 0$ is the spatial frequency, and $r^2 = x^2 + z^2$. We assume all layers are half plane and neglect finite thickness.

From the block diagrams and relations, transfer functions are calculated for both systems. With no lubricant between the rubber layers (complete shear stress information transmitted), the overall frequency response for the teletaction system is:

$$\begin{aligned}H_s(s, z = d_1 + d_2) &= \frac{\mathcal{F}[\epsilon_z(x, z = d_1 + d_2)]}{\mathcal{F}[\sigma_z(x, z = 0)]} \\ &= \frac{1}{E}e^{-2\pi(d_1+d_2)s}(\frac{1}{2} + 3\pi(d_1 + d_2)s)\end{aligned}$$

where $\mathcal{F}$ is the Fourier transform.

With lubricant between the rubber layers (no shear stress information transmitted), the overall frequency response for the teletaction system is:

$$\begin{aligned}H_{ns}(s, z = d_1 + d_2) &= \frac{\mathcal{F}[\epsilon_z(x, z = d_1 + d_2)]}{\mathcal{F}[\sigma_z(x, z = 0)]} \\ &= \frac{1}{E}e^{-2\pi(d_1+d_2)s}(\frac{1}{2} + \pi(d_1 + 3d_2)s + 6\pi^2 d_1 d_2 s^2)\end{aligned}$$

In our case, we set $d_1 = 1.0$ mm and $d_2 = 1.7$ mm (1.0 mm for the second rubber layer and 0.7 mm for approximate depth of the mechanoreceptors in the skin). The normalized frequency responses, found by multiplying $H_s(s, z)$ and $H_{ns}(s, z)$ by E, are plotted in Figure 5.

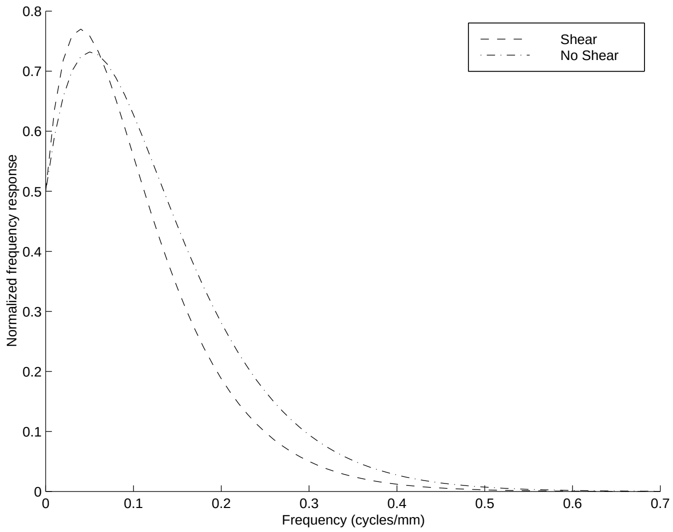

Figure 5: Normalized frequency responses when $d_1 + d_2 = 2.7$ mm

Normal Strain Profile based on Displacement Profiles

The systems above predict the normal strain profile given the input normal stress profile. Since we actually have a displacement profile input from the gratings, we need to find the equivalent set of line loads corresponding to a given displacement profile. We follow the procedure of Phillips and Johnson (1981) as detailed in the Appendix.

Given a deflection profile corresponding to a 4.0 mm period grating indenting 2.0 mm, as shown in Figure 6a, we calculate a line load profile that would produce this deflection profile. Knowing that the normal stress is zero where there is no contact with the grating, and limiting our surface normal stress to have only compressive components, we are left with a surface normal stress profile, $\sigma_z(x)$, shown in Figure 6b. The deflection profile corresponding to $\sigma_z(x)$ can be found by convolving $\sigma_z(x)$ and $c(x)$, as defined in the Appendix, and is shown in Figure 6c.

From the surface normal stress, we can calculate the normal strain profile, $\epsilon_z(x)$, for the two different systems shown in Figure 4. A modulation index is calculated for each of the normal strain profiles. The normal strain profile from -10 mm to 10 mm (to avoid the edge effects) can be approximately represented as

$$\epsilon_z(x) \sim \alpha(1 + \mu\cos(\omega x))$$

where α is a scaling constant, ω is the frequency of the grating, and μ is the modulation index. The two normal strain profiles are shown in Figure 7. As predicted by the transfer functions, the modulation index when no shear information is transmitted is higher than when shear information is transmitted. Figure 8

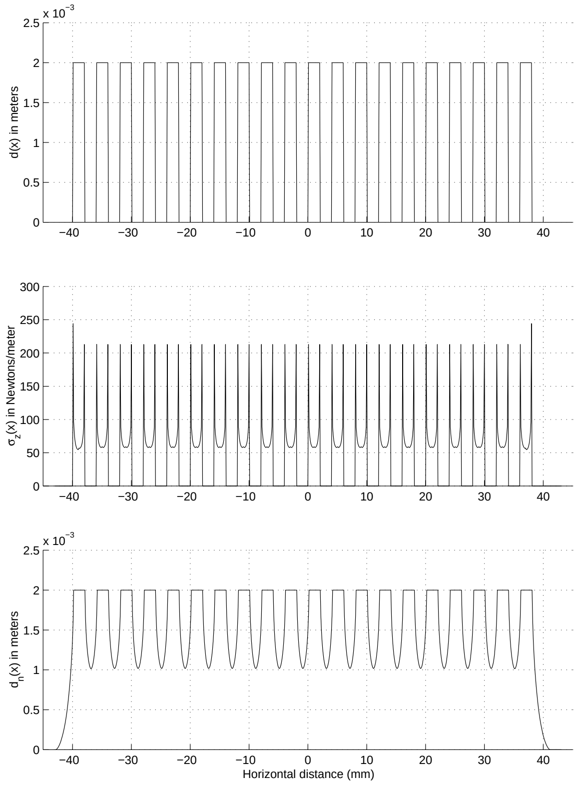

Figure 6: a) Displacement profile applied, b) Surface normal stress, and c) Displacement profile calculated by convolving normal stress in b) with the c(x) of Figure 13

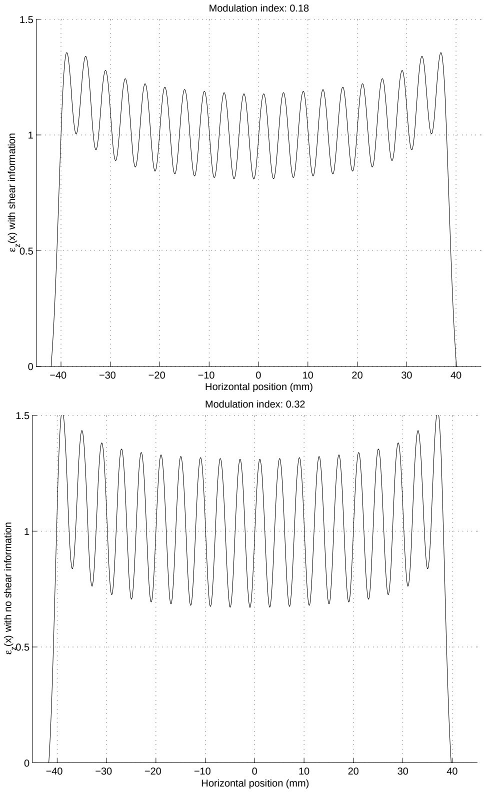

Figure 7: The two normalized normal strains and modulation indices at a depth of 2.7 mm due to a 4.0 mm periodic grating pattern

shows the modulation indices as a function of the grating frequency used as input. Note that with a 2.7 mm thick low pass layer, the grating frequencies of 0.2 to 0.5 cycles/mm contain information mostly at the fundamental frequency. The higher harmonics are greatly attenuated as shown in the frequency response (Figure 5).

With an SA I mechanoreceptor density of about 1 mm^{-1}, the highest frequency that can be accurately perceived is a 0.5 cycle/mm grating by the Nyquist sampling criterion. Grating experiments on the bare finger by Phillips and Johnson (1981) found that 2.0 mm is the minimum detectable spatial resolution for orientations. Theoretically, at a sufficiently high modulation index, all subjects should be able to perfectly discriminate orientations. At a sufficiently low modulation index, subjects should not be able to discriminate due to noise in the tactile perception system, rather than insufficient sampling density. With lubricated elastic layers, we predict that gratings of the same period will have a higher modulation index. The increased modulation index should correlate with better orientation discrimination. Thus, with lubricated elastic layers, higher frequency gratings should be better detected.

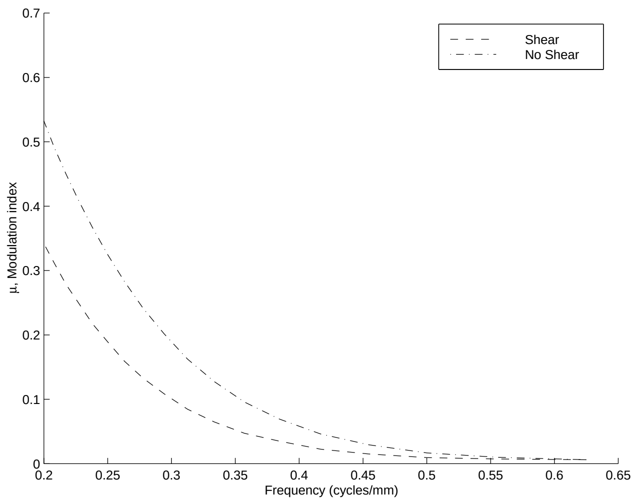

Figure 8: Modulation index vs. frequency

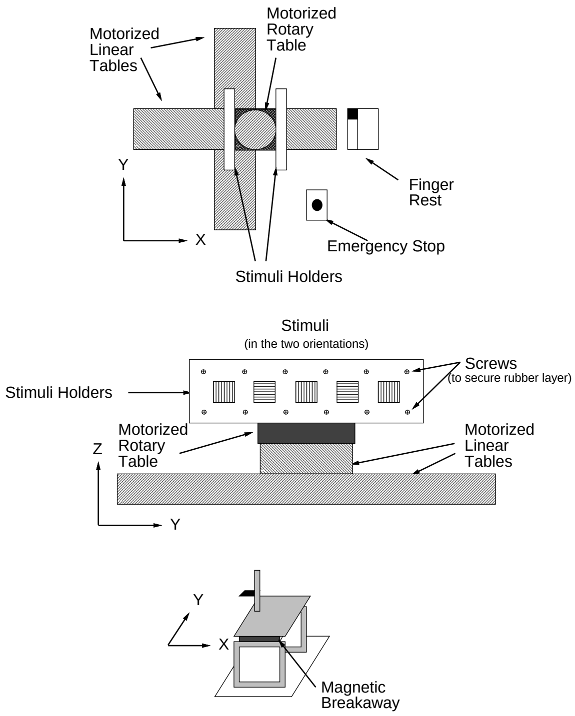

Figure 9: Testing apparatus: a) Top view of overall setup, b) Front view of the tables, stimuli holder, and stimuli, c) Side view of the finger rest

EXPERIMENTAL METHODS

To test the thresholds of human tactile resolution with and without the transmission of shear stress information, we built a system which presents stimuli with different spatial frequencies and orientations and allows the two different rubber layers to be easily exchanged. The system provides accurate position control repeatability.

Apparatus

We developed a system that allows us to quickly present stimuli patterns to the subject in an accurate manner. The motion control was provided by two motorized linear tables and one motorized rotary table, configured in the x, y, and θ orientation shown in Figure 9a. The motorized tables were controlled by a Pentium based PC running Windows NT 4.0. The control program recorded the subjects' responses.

Two stimuli holders with 10 stimuli were bolted onto the rotary table (Figure 9b). Wax blocks with horizontal or vertical grating patterns were placed into the holders. The grating patterns had periods ranging from 2.4 mm to 4.8 mm in 0.6 mm increments with a 50% duty cycle. This narrow range of periods was based on the results of Tan (1995). The rubber layer was either a solid 2 mm silicone rubber sheet or two 1 mm silicone rubber sheets with a thin layer of lubricant in between. We used a vegetable oil spray, PAM[2], as the lubricant as other lubricants we tried either dried up too quickly or reacted unfavorably with the silicone rubber. The 2 mm thickness for the rubber layer was used based on having an actuator array with 2 mm spacing between the actuators. The 1:1 ratio of spacing and layer thickness gives good anti-aliasing characteristics and an acceptable signal to noise ratio (Fearing et al 1997).

The subject's right index finger was placed in a position such that the presented stimuli would come into contact normally with the fingerpad. It was essential that no extraneous information was given to the subject by having the stimuli contact obliquely and slide across the finger when coming to the final contact position. Two safety devices were incorporated into the design of the system. An emergency stop button was located in an easily accessible place which would immediately stop all motion of the motor tables. The other safety device was a magnetic breakaway located on the finger rest. Subjects were instructed to look away from the apparatus but not blindfolded so that in case of emergency, the subject could quickly determine the best plan of action to avoid injury.

Procedure

Our goal was to measure change in tactile spatial sensitivity without the transmission of shear stress information. Therefore, we designed experiments that measured the threshold of orientation detection with and without the shear stress information.

The experiment consisted of two trials. For the anti-aliasing spatial low-pass filter, one trial used a solid 2 mm silicone rubber sheet and the other trial used two 1 mm silicone rubber sheets with a thin layer of PAM in between. It was randomly decided which trial was performed first.

In each of the trials, the subject extended their right index finger and placed it on the finger rest (Figure 9c). The finger rest was adjusted to insure that contact with the stimuli would occur in the normal direction of the fingerpad. Then the subject chose a comfortable indentation level which gave optimum sensitivity. Most subjects used 10 practice trials to find the optimum sensitivity. The average force applied to the finger was 10 N. The setup was calibrated with a dial indicator to insure that each stimulus would indent to the chosen distance with error of less than 25 μm. The control program then presented each of the ten stimuli fifteen times in a random order. Of the ten stimuli, there were 5 distinct frequencies tested in both orientations. This resulted in thirty points per frequency tested with half of the points in each orientation.

After the control program presented the stimuli, the subject responded with a "0" or "1" corresponding to which orientation was felt (Figure 10). The trial was then repeated with the other rubber layer. Each trial took approximately 30 minutes and could be completed on different days, if necessary.

Friction coefficients

We measured friction coefficients between rubber and wax, and two sheets of rubber, with and without the lubricant. A

[2] American Home Products, Inc.

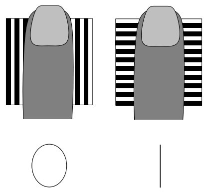

Figure 10: Subjects' response for perceived orientation

Materials	Friction Coeff.
Rubber/wax	1.4
Rubber/Rubber (no lubricant)	2.7
Rubber/Rubber (lubricant)	0.1

TABLE 1: Measured coefficients of friction

mass was placed on top of the materials being tested. Measuring the horizontal force needed to move the rubber gives the friction coefficient. As shown in Table 1, there is a significant decrease in friction with the lubricant. The low friction between the lubricated layers corresponds to a reduction of $\tau_{xz}(x, z = d_1)$ applied to the second elastic layer (Figure 4b). We assume only the normal stress profile, $\sigma_z(x, z = d_1)$ is transmitted to the second elastic layer.

RESULTS

The experiments were run on 10 human subjects (9 male, 1 female). All subjects were volunteers, and two subjects were familiar with the experimental procedure and apparatus. The subjects' results are shown in Table 2. Graphs of the data are shown in Figure 11 with error bars showing 95% confidence intervals for a proportion with 30 trials. We ignored subject to subject variations and averaged the data from all ten subjects (Figure 12).

Looking at the data, we see that there was better orientation discrimination with reduced shear information. To quantify the significance, we applied the χ^2 test with 1 degree of freedom (Walpole and Myers, 1993). We use the average as the expected frequency.

The calculated χ^2 values are as follows:

Period (mm)	2.4	3.0	3.6	4.2	4.8
χ^2	2.41	4.98	7.29	34.3	28.7

The results of the shear and reduced shear experiments are from different populations for grating periods greater than or equal to 3.0 mm (95% probability, $\chi^2 > 3.84$). Since 2.4 mm was below the detectable threshold with a 2.7 mm thick anti-aliasing layer, it is not surprising that there was no significant difference between the shear and reduced shear data. Tan [1995] presented flat and grating patterns to determine at which frequency subjects could discriminate a flat pattern from a grating

Shear					
Period (mm)	2.4	3.0	3.6	4.2	4.8
Subject 1:	12	15	23	28	29
Subject 2:	20	16	16	22	26
Subject 3:	13	14	11	21	22
Subject 4:	17	15	17	23	12
Subject 5:	17	15	18	27	23
Subject 6:	13	22	18	25	26
Subject 7:	13	15	15	18	21
Subject 8:	12	18	15	25	27
Subject 9:	15	15	20	23	28
Subject 10:	7	15	19	18	20
Mean	13.9	16.0	17.2	23.0	23.4

Reduced Shear					
Period (mm)	2.4	3.0	3.6	4.2	4.8
Subject 1:	12	21	24	26	30
Subject 2:	21	15	15	30	29
Subject 3:	20	17	15	30	28
Subject 4:	17	27	27	27	30
Subject 5:	16	18	18	29	30
Subject 6:	14	28	21	28	25
Subject 7:	15	15	15	26	26
Subject 8:	14	14	24	30	29
Subject 9:	16	18	23	29	28
Subject 10:	13	14	22	26	25
Mean	15.8	18.7	20.4	28.1	28.0

TABLE 2: Raw data from experiments. Data are number correct out of 30 trials per period per subject

pattern through a 2 mm glove. The average grating period for 75% correct discrimination was 4.0 mm. This closely agrees with our results (Figure 12).

DISCUSSION AND CONCLUSION

The increase in spatial resolution with reduced shear is consistent with the increase in modulation index for the frequencies of interest (Figure 8). For tractable analysis, we assumed a frictionless normal indentation of the stimuli onto the elastic layers. Even though there is a frictionless indentation at the surface, there is a subsurface shear stress at the intermediate boundary. When shear is removed on the intermediate boundary, the model predicts an increase in modulation indices, and the experiments confirm that at the frequencies tested, the percentage correct was always greater when there was reduced shear stress information transmitted between the elastic layers.

If we assume that each subject has a threshold period, then the tactile spatial resolution should be improved by reducing the shear stress information. This idea is put to practice in the Sensopad, a device which aids in breast self examinations. It is con-

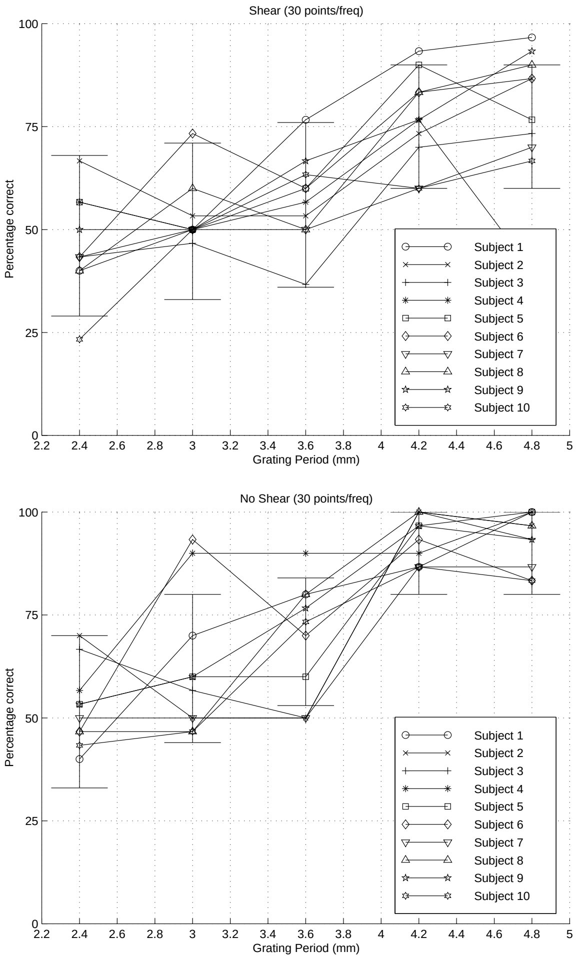

Figure 11: Graphs of the data with error bars representing the 95% confidence intervals for a proportion. Each point represents the results of 30 trials.

structed by placing silicone fluid in between two layers of silicone rubber. Its claim of enhancing the perception of small embedded objects agrees with our results. From system theory, we know that the only information needed to characterize a linear space-invariant system is the frequency response. By using gratings as the stimuli, and determining the lowpass filter characteristics of the rubber layers, we calculated the associated transfer function and frequency response. For static contact, lumps can be thought of as a weighted sum of gratings, thus detecting small lumps corresponds to detecting high frequency gratings.

In previous work, we compared the normal subsurface strain with and without shear information transmitted at the boundary layer (Fearing et al 1997). We found that the distortion caused by removing shear information caused a 16 dB discrepancy between the strain profiles. For gratings, this distortion increased the modulation index, which told us that the discrepancy amplified the periodic components of the normal strain profile. Shear information might be important in sensing and reconstructing

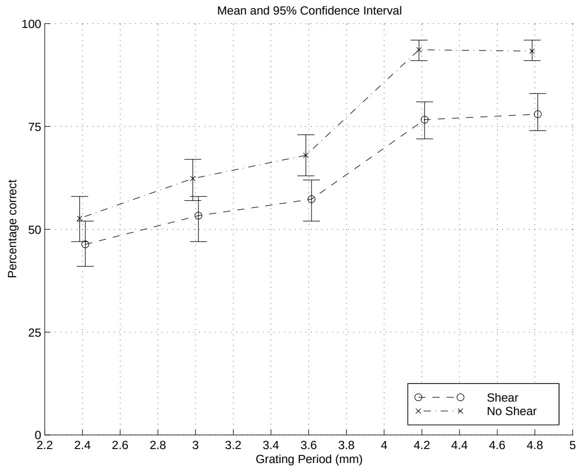

Figure 12: Averages of the data from 10 subjects. Each point represents the results of 300 trials.

other classes of contacts, but not normal frictionless contacts.

In designing a teletaction system, it is important to consider what type of contacts the sensor will encounter. If the sensor operates in an environment where contact is composed of mainly normal stresses, the reduction of shear stress information can be beneficial by enhancing the higher frequency information present in subsurface skin strain. An example of such an environment is laparoscopic surgery with tactile sensors on the ends of the instruments. Contact with organs will be low friction contacts due to the slipperiness of the organs. This leads to a contact where normal stresses are high compared to tangential stresses. In these environments, a tactile display using an array of 1 DOF actuators should be as effective as using an array of 3 DOF actuators.

Future Work

Future work in this area includes allowing subjects to scan the stimuli, using better models of the finger/elastic layer/stimuli interaction, and testing stimuli with a tangential stress component. Refinement of our apparatus will include integrating a force/torque sensor to give a more consistent presentation of stimuli.

ACKNOWLEDGMENTS

We thank K. Chiang, J. Yan, W. Zesch, J. Hsu, and A. Mazaheri for helpful discussions and comments.

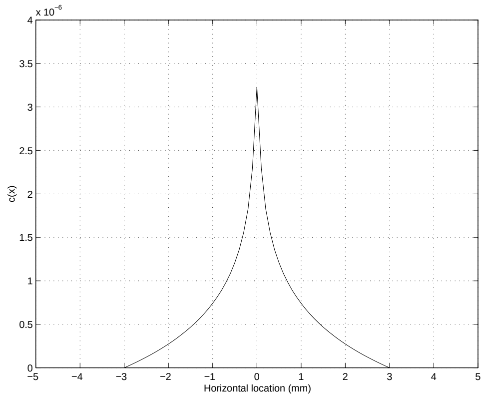

Figure 13: Deflection profile, c(x), caused by a line load at $x = 0$ with $x_0 = 25$ μ m and $x_b = 3.0$ mm

APPENDIX

The fundamental relation between a surface deflection and a normally applied line load is shown in Figure 13, and given by:

$$c(x) = \begin{cases} \frac{2}{\pi E} log \frac{x_b}{x_o}, & |x| < x_o \\ \frac{2}{\pi E} log \frac{x_b}{x}, & x_o < |x| < x_b \\ 0, & x_b < |x| \end{cases} \quad (1)$$

where x_0 is half the width of the applied line load, and x_b is the distant boundary. So from equation 1, the line load has a constant deflection in the width of application, decays logarithmically until the distant boundary, and is zero outside of the distant boundary. We used the same values as Phillips and Johnson (1981) and Tan (1995), $x_0 = 25$ μm and $x_b = 3$ mm.

As in Phillips and Johnson (1981), we assume that the deflection is proportional to the magnitude of the line load, the deflection function c(x) is space invariant, and the overall deflection profile is the superposition of deflection profiles from the individual line loads. Discretizing c(x), we can represent the discretized deflection profile d(x_i) as:

$$d(x_i) = \sum_{j=1}^{n} c(x_i - x_j) p(x_j) \quad (2)$$

where $p(x_j)$ is the discretized line load profile, and n is the number of points representing the profiles. Rewriting equation 2 least squares problem. Given a deflection profile d and the deflection matrix C (calculated from c(x)), we can find p as follows:

$$Cp = d \quad (3)$$

$$p = (C^T C)^{-1} C^T d \quad (4)$$

In our case, p and d are the same length, so

$$p = C^{-1} d \quad (5)$$

REFERENCES

[1] D.J. Beebe, C.M. Hymel, K.A. Kaczmarek, M.E. Tyler, "A polyimide-on-silicon electrostatic fingertip tactile display", *IEEE Engineering in Medicine and Biology 17th Annual Conference and 21 Canadian Medical and Biological Engineering Conference*, vol. 2, pp. 1545-6, Montreal, Que., Canada, Sept. 1995.

[2] M. Cohn, M. Lam, and R. Fearing, "Tactile Feedback for Teleoperation", *SPIE Telemanip. Tech.*, vol. 1833, pp. 240-254, 1992.

[3] R.S. Fearing, G. Moy, E. Tan, "Some Basic Issues in Teletaction", *IEEE Int. Conf. on Rob. and Auto.*, vol. 4, pp. 3093-9, Albuquerque, April 1997.

[4] H. Fischer, B. Neisius, and R. Trapp, "Tactile Feedback for Endoscopic Surgery", *Interactive Technology and New Paradigm for Healthcare* , ed: K. Morgan, R.M. Satava, H.B. Sieburg, R. Mattheus, J.P. Christensen, pp. 114-117, IOS Press 1995.

[5] R. Ghodssi, D.J. Beebe, V. White, and D.D. Denton, "Development of a Tangential Tactor Using a LIGA/MEMS Linear Microactuator Technology", 1996 Int. Mech. Eng. Cong. and Exposition, Microelectromechanical Systems, DSC vol. 59, pp. 379-386, Nov. 17-22, 1996.

[6] C.J. Hasser and M.W. Daniels, "Tactile Feedback with Adaptive Controller for a Force-Reflecting Haptic Display", 15th Southern Biomedical Engineering Conf., pp. 526-533, Dayton, OH, 29-31 March 1996.

[7] R.D. Howe, W.J. Peine, D.A. Kontarinis, and J.S. Son, "Remote Palpation Technology", *IEEE Eng. in Med. and Bio. Mag.*, pp. 318-323, May/June 1995.

[8] K.A. Kaczmarek, J.G. Webster, P. Bach-y-Rita, and W.J. Tompkins, "Electrotactile and Vibrotactile Displays for Sensory Substitution Systems", *IEEE Trans. on Bio. Eng.*, vol. 38, no. 1, pp. 1-16, January 1991.

[9] K.L. Johnson, *Contact Mechanics*, Cambridge University Press, 1985.

[10] S.J. Lederman, "Heightening tactile impressions of surface texture", *Active Touch*, ed. G. Gordon. Oxford: Pergamon Press, pp. 205-214, 1978.

[11] J.M. Loomis and S.J. Lederman, "Tactual Perception", in *Handbook of Perception and Human Performance*, edited by K.R. Boff, L. Kaufman and J.P. Thomas, pp. 31-1:31-41, John Wiley and Sons: New York, 1986.

[12] J.R. Phillips and K.O. Johnson, "Tacile Spatial Resolution II. Neural Representation of Bars, Edges, and Gratings in Monkey Primary Afferents", *J. Neurophysiology*, vol. 46, no. 6, pp. 1192-1203, 1981.

[13] J.R. Phillips and K.O. Johnson, "Tacile Spatial Resolution III. A Continuum Mechanics Model of Skin Predicting Mechanoreceptor Response to Bars, Edges, and Gratings", *J. Neurophysiology*, vol. 46, no. 6, pp. 1204-1225, 1981.

[14] M. Shimojo, M. Shinohara, and Y. Fukui, "Human Shape Recognition Performance for 3D Tactile Display", *IEEE International Conference on Systems, Man, and Cybernetics*, vol.4, pp. 3192-7, Orlando, FL, USA, 12-15 Oct. 1997.

[15] U. Singh, "Temporal Characteristics of the Human Finger" Master's Report, Dept of EECS, UC Berkeley, May 1997.

[16] M.A. Srinivasan and K. Dandekar, "An Investigation of the Mechanics of Tactile Sense Using Two Dimensional Models of the Primate Fingertip" *I Jnl. of Biomechanical Engineering (trans. of the ASME)*, vol. 118, pp. 48-55, 1996.

[17] E. Tan, "Estimating Human Tactile Resolution Limits for Stimulator Design", Master's Report, Dept of EECS, UC Berkeley, May 1995.

[18] R. Walpole and R. Myers, *Probability and Statistics for Engineers and Scientists.* Macmillan Publishing Company, 1993.